

A comparative study of Photocatalytic degradation of Azure-B by tungsten containing nanoparticles: sunlight used as energy source

Ankita Vijay¹, Shipra Bhardwaj²

¹Mewar university, Gangrar Chittorgarh (Rajasthan) India

²Government Meera Girls College, Udaipur (Rajasthan) India

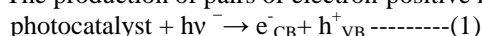
Abstract: The waste water from the textile industries generate serious problems for environment by the presence of color compounds such as dyes and these are resistant to the natural and conventional treatment. Present work incorporates the photocatalytic degradation of Azure-B dye using tungsten containing semiconductors (WO_3 , $BaWO_4$ and $Ba_3Y_2WO_9$) and solar light. The degradation of dye in aqueous solution was examined spectrophotometrically. It was observed that concentrations of dye, pH, amount of semiconductor, intensity of light were significant parameters whose influence is directly related to changes in the concentration of OH and O_2^- free radicals.

Keywords: Photocatalyst, Scavenger, Pseudo first order reaction, Intensity of light.

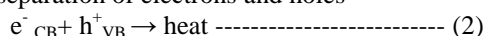
I. Introduction

Dyes are usually resistant compounds that can be found industrial wastewater, producing drastic environmental problems [1]. Different biological treatments [2] and traditional methods like ultra filtration, extraction and carbon adsorption [3] have been applied to remove such compounds. A disadvantage of most of these processes is that they are non-destructive; they simply transfer the pollutant from one phase to another [4]. Over the past few years, several advanced oxidation processes (AOPs) have been proposed as alternative routes for water purification. Among them, oxidation via ozonolysis or hydrogen peroxide was one method [5]. Nevertheless, the photocatalytic process seems to be the most successful one for water decontamination, since it involves strong oxidizing species such as hydroxyl radicals [6,7]. The photocatalytic degradation rate of different compounds depend on various parameters (concentration of semiconductor, initial concentration of the pollutant, initial pH, temperature, light intensity, addition of salts and oxidants, partial pressure of oxygen, etc.) [8, 9]. A photocatalytic process is based on the action of light on the surface of a semiconductor, which causes a jump of electrons from the valence band to the conduction band (electronically). This process can be summarized, in brief, in three steps:

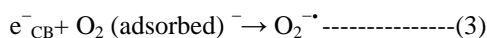
- (1) The production of pairs of electron-positive holes[10]



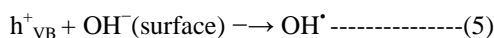
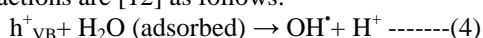
- (2) The separation of electrons and holes



Recombination of electrons and holes is the main factor limiting the rate of oxidation of organic substrates [11]. The recombination should be thus avoided, for an efficient photocatalyst. This is made possible by the transfer and trapping of free charges to intermediate energy level (irregularities of structure or adsorbed molecules). For example, the electron trapping occurs through molecular oxygen adsorbed, forming superoxide radicals.



- (3) The oxidation and reduction: the charges created migrate to the surface of the catalyst and react with adsorbed substances likely to accept electrons (i.e. oxidizing) or give electrons (i.e. reducing). These are oxidation or reduction substances which are interesting for remediation. Thus, in an aqueous medium, the hydroxyl groups OH, adsorbed on the surface of photocatalyst, react and produce free radicals OH $^{\cdot}$. In fact, the main reactions are [12] as follows:



Tungsten materials with novel architectures and physical and chemical properties are very useful for many potential applications such as flashing materials, LED [13], magnetic and fluorescent materials [14-20],

optical fiber, humidity sensors [21], light emitting materials [22,23], photocatalytic materials [24-30], scintillator [31], laser host[32], and nanoordered substrate materials[33,34], so they are considered as an important class of functional materials. As important photocatalyst tungsten containing semiconductor (WO_3 , BaWO_4 and $\text{Ba}_3\text{Y}_2\text{WO}_9$) has been applied for photodegradation of Azure B dye from water under solar light irradiation.

II. Materials And Methods

Stock solutions of Azure B dye ($0.030583\text{g}/100\text{ ml}=1\times 10^{-3}\text{M}$) was prepared in doubly distilled water and diluted as required. The optical density (O.D.) of the solution at $\lambda_{\text{max}} = 648\text{ nm}$ was determined using a spectrophotometer (Systronics Model 106). The pH of the solution was varied by prestandardized NaOH and HCl solutions and was determined by pH meter (Heraeus pen type). To 50 ml of the solution, 0.10 g of Tungsten oxide, 0.18 g of Barium tungstate and 0.12 g of Barium yttrium tungsten oxide was added respectively and it was exposed to a 200 watt tungsten lamp (Philips). The O.D. of the solution was recorded at different time intervals and graph was plotted between time and $1+\log \text{O.D.}$ It was found to be a straight line suggesting the reaction to follow pseudo first order kinetics. The rate constant was determined by –
 $K=2.303 \times \text{slope}$

A water filter was used to cut off the heat reaction. Use of scavenger suggested the participation of OH^{\cdot} free radical in the reaction. This free radical is found to be strong enough to break the different bond of dye (C=N, C-N, C=C, C-C, C-S etc). Controlled experiments proved the reaction neither photo degradation nor catalytic degradation rather it was a photo catalytic degrading process.

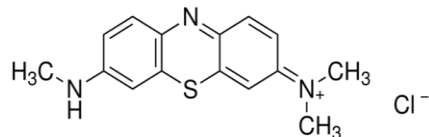


Fig. 1: Structure of Azure B

III. Results And Discussion

3.1 A typical run

To a 100mL beaker, 50mL of dye solution was added, 0.12, 0.18 and 0.12g of semiconductors WO_3 , BaWO_4 and $\text{Ba}_3\text{Y}_2\text{WO}_9$ were added respectively and the setup was covered with water filter to avoid heat reaction. This assembly was exposed to 200 watt tungsten lamp. At different time intervals an aliquot of 2mL was taken out and the optical density (O.D.) was recorded. It was observed that the O.D. of solution decreases with time.

The data of typical run for all the three semiconductors are given in Figures (Figure 6 for WO_3 and Azure B, Figure 7 for BaWO_4 and Azure B and Figure 8 for $\text{Ba}_3\text{Y}_2\text{WO}_9$) and Table 1. It is observed from the comparison of data that efficiency of ternary semiconductor to remove the dye is much greater than other two semiconductors.

3.2 Effect of pH

The effect of variation of pH on the rate of photocatalytic degradation of Azure B was investigated by keeping all other factors constant and by varying the pH of the solution by adding prestandardized HCl and NaOH solutions. The data are represented graphically in Figure 2 and comparison is reported in Table 2. The rate of photocatalytic degradation of Azure B increases for the WO_3 , BaWO_4 and $\text{Ba}_3\text{Y}_2\text{WO}_9$ with increase in pH up to a pH value of 7.8, 7.3 and 7.3 respectively and then decreases again with increase in pH value above 7.8 and 7.3. This behavior may be explained on the basis that the increase in the rate of photocatalytic degradation may be due to the increased availability of OH^- at higher pH values. By combining with holes, OH^- ions will generate more hydroxyl radicals (OH^{\cdot}) which are considered responsible for the photocatalytic degradation. Above a pH value of 7.3 or 7.8, the increased number of OH^- ions will compete with the electron rich dye. The OH^- ions will make the surface of the semiconductor negatively charged and as a consequence of repulsive force between two negatively charged species (OH^- ions and the electron rich dye) the approach of Azure B molecules to the semiconductor surface will be retarded. This will result in a decrease in the rate of photocatalytic degradation of Azure B dye.

3.3 Effect of dye concentration

It is important both from a mechanistic and from an application point of view to study the dependence of the photocatalytic reaction rate on the substrate concentration. Thus the effect of concentration of dye was observed on the rate of reaction by changing the concentration of dye and by keeping all other factors constant. The data are represented graphically in Figure 3 and compared in table 2. It is generally noted that the

degradation rate increases with the increase in dye concentration to a certain level and a further increase in dye concentration leads to decrease the degradation rate of the dye. The rate of degradation relates to the probability of OH⁻ radicals formation on the catalyst surface and to the probability of OH⁻ radicals reacting with dye molecules. As the concentrations of the dye increase the probability of reaction between dye molecules and oxidizing species also increases, leading to an enhancement in the decolorization rate. On the contrary, the degradation efficiency of the dye decreases as the dye concentration increases further. The presumed reason is that at high dye concentrations the generation of OH⁻ radicals on the surface of catalyst are reduced since the active sites are covered by dye ions. Another possible cause for such results is the Visible-screening effect of the dye itself. At a high dye concentration, a significant amount of light may be absorbed by the dye molecules rather than the semiconductor particles and that reduces the efficiency of the catalytic reaction because the concentrations of OH⁻ and O₂⁻ is decreased.

3.4 Effect of amount of semiconductor

The effect of variation of semiconductor on the rate of the photocatalytic degradation of the Azure B was also recorded and all other factors were kept constant. The results are given graphically in Figure 4 and are compared in Table 2. The value of K increases with increase in the amount of WO₃ (0.12g), BaWO₄ (0.18g), Ba₃Y₂WO₉ (0.12g). Beyond the particular amount of semiconductor, the rate of the photocatalytic degradation decreases as the amount of the semiconductor increases. It is likely to state that addition of semiconductor increases the site to absorb the light and generate electron hole pair. This increases the rate of degradation. Beyond the particular amount of semiconductor, the further addition increases the thickness of the semiconductor layer without affecting its surface area. Further, addition of semiconductor may generate more number of OH⁻ and the caused crowd may repel the oxidizing species forcing their recombination with holes and thus reduction in rate is observed.

3.5 Effect of light intensity

The effect of variation of light intensity on the rate of photocatalytic degradation of Azure B was observed by keeping all other variables constant. The results obtained are reported graphically in Figure 5 and are compared in Table 2. The observation shows that an increase in light intensity increases the rate of photocatalytic degradation. As the intensity of light increases, the number of photons striking per unit area of the semiconductor (WO₃< BaWO₄< Ba₃Y₂WO₉) also increases. A linear behavior between light intensity and the rate of reaction was observed. Since an increase in the light intensity increases the temperature of dye solution and a thermal reaction may occur, therefore higher intensities were avoided.

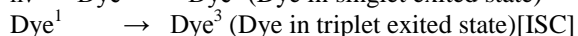
IV. Conclusion

It is concluded here that the rate of degradation of dye molecule in water is affected by following factors:

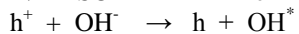
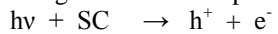
- A. pH of the solution
- B. Concentration of the dye
- C. Amount of the semiconductors
- D. Intensity of light
- E. Type of semiconductor

A mechanism is proposed:

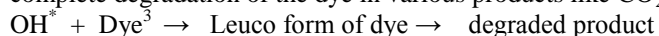
As light falls on the dye it gets excited to its singlet state and then by loosing energy through inter system crossing gets converted to triplet state.



On the other hand semiconductor, on exposure to light generates an electron hole pair by exciting an electron from highest occupied molecular orbital (HOMO) to lowest unoccupied molecular orbital (LUMO) and generating a hole. In photo oxidation process this hole is responsible which abstracts an electron from OH⁻ ion and generates the responsible OH^{*} free radical species.



These free radicals attack the dye molecule, break its conjugation starting a chain reaction which causes a complete degradation of the dye in various products like CO₂, H₂O, NO₂, H₂S, SO₂ etc. gases.



These gases are removed from water, making it safe for further use.

A comparative study (Table 2) of all the semiconductors show the supremacy of ternary semiconductor as it requires less time to degrade the dye, less amount of semiconductor is required and pH of the solution is less altered thus causing less alteration to the environmental factors.

References

- [1]. A. Bianco Prevot, C. Baiocchi, M. Brussino, E. Pramauro, P. Savarino, V. Augugliaro, et al., Photocatalytic degradation of Acid Blue 80 in aqueous solutions containing TiO₂ suspensions, Environmental Science & Technology, 35, 2001, 971–976.
- [2]. I. M. Banat, P. Nigam, D. Singh, and R. Marchant, Microbial decolorization of textile-dye-containing effluents: A review, Bioresearch Technology, 58, 1996, 217–227.
- [3]. A. S. Ozcan, B. Erdem, and A. Ozcan, Adsorption of Acid Blue 193 from aqueous solutions onto Na-bentonite and DTMA-bentonite, Journal of Colloid Interface Science, 280, 2004, 44–54.
- [4]. S. S. Tahir and N. Rauf, Removal of a cationic dye from aqueous solutions by adsorption onto bentonite clay, Chemosphere, 63, 2006, 1842–1848.
- [5]. W. G. Kuo, Decolorizing dye wastewater with Fenton's reagent, Water Research, 26, 1992, 881–886.
- [6]. H. Lachheb, E. Puzenat, A. Houas, M. Ksibi, E. Elaloui, C. Guillard, Photocatalytic degradation of various types of dyes (Alizarin S, Crocein Orange G, Methyl Red, Congo Red, Methylene Blue) in water by UV-irradiated titania, Applied Catalysis B, 39, 2002, 75–90.
- [7]. P. C. Vandevivere, R. Bianchi, and W. Verstraete, Review: Treatment and reuse of wastewater from the textile wet-processing industry: Review of emerging technologies, Journal of Chemical Technology Biotechnology, 72, 1998, 289–302.
- [8]. L. Chen, Effects of factors and interacted factors on the optimal decolorization process of Methyl Orange by ozone, Water Research, 34, 2000, 974–982.
- [9]. F. Kiriakidou, D. I. Kondarides and X. E. Verykios, The effect of operational parameters and TiO₂-doping on the photocatalytic degradation of azo-dyes, Catalysis Today, 54, 1999, 119–130.
- [10]. J.-M. Herrmann, Heterogeneous photocatalysis: fundamentals and applications to the removal of various types of aqueous pollutants, Catalysis Today, 53, 1999, 115–129.
- [11]. M. R. Hoffmann, S. T. Martin, W. Choi, and D. W. Bahnemann, Environmental applications of semiconductor photocatalysis, Chemical Reviews, 95, 1995, 69–96.
- [12]. [12] S. Wen, J. Zhao, G. Sheng, J. Fu, and P. Peng, Photocatalytic reactions of phenanthrene at TiO₂/water interfaces, Chemosphere, 46, 2002, 871–877.
- [13]. E. Tomaszewicz, S. M. Kaczmarek, and H. Fuks, New cadmium and rare earth metal tungstates with the scheelite type structure, Journal of Rare Earths, 27(4), 2009, 569–573.
- [14]. S. J. Chen, J. H. Zhou, X. T. Chen, Fabrication of nanocrystalline ZnWO₄ with different morphologies and sizes via hydrothermal route, Chemical Physics Letters, 375, 2003, 185–190.
- [15]. V. B. Mikhailik, H. Kraus, D. Wahl, M. Itoh, M. Koike, and I. K. Bailiff, One- and two-photon excited luminescence and band-gap assignment in CaWO₄, Physical Review B, 69(20), 2004, 9.
- [16]. D. Chen, G. Z. Shen, K. B. Tang, H. G. Zheng, and Y. T. Qian, Low-temperature synthesis of metal tungstates nanocrystallites in ethylene glycol, Materials Research Bulletin, 38, 2003, 1783–1789.
- [17]. X. Jiang, J. Ma, J. Liu, Synthesis of ZnWO₄ nano-particles by a molten salt method, Materials Letters, 61(23-24), 2007, 4595–4598.
- [18]. E. Cavalli, A. Belletti, and M. G. Brik, Optical spectra and energy levels of the Cr³⁺ ions in MWO₄(M = Mg, Zn, Cd) and MgMoO₄ crystals, Journal of Physics and Chemistry of Solids, 69(1), 2008, 29–34.
- [19]. M. Itoh, T. Katagiri, T. Aoki, and M. Fujita, Photo-stimulated luminescence and photo-induced infrared absorption in ZnWO₄, Radiation Measurements, 42(4-5), 2007, 545–548.
- [20]. [20]A. Kalinko, A. Kuzmin, and R. A. Evarestov, Ab initio study of the electronic and atomic structure of the wolframite-type ZnWO₄, Solid State Communications, 149(11-12), 2009, 425–428.
- [21]. W. M. Qu, W. Włodzki, and J. U. Meyer, Comparative study on micromorphology and humidity sensitive properties of thin-film and thick-film humidity sensors based on semiconducting MnWO₄, Sensors and Actuators B, 64, 2000, 76–82.
- [22]. Q. L. Dai, H. W. Song, X. Bai, Photoluminescence properties of ZnWO₄: Eu³⁺ nanocrystals prepared by a hydrothermal method, Journal of Physical Chemistry C, 111, 2007, 7586–7592.
- [23]. J. Wu, F. Duan, Y. Zheng, and Y. Xie, Synthesis of Bi₂WO₆ nanoplate-built hierarchical nest-like structures with visible-light-induced photocatalytic activity, Journal of Physical Chemistry C, 111(34), 2007, 12866–12871.
- [24]. J. Lv, Z. Zhao, Z. Li, J. Ye, and Z. Zou, Preparation and photocatalytic property of LiCr(WO₄)₂, Journal of Alloys and Compounds, 485, 2009, 346–350.
- [25]. H. B. Fu, J. Lin, L. W. Zhang, and Y. F. Zhu, Photocatalytic activities of a novel ZnWO₄ catalyst prepared by a hydrothermal process, Applied Catalysis A, 306, 2006, 58–67.
- [26]. H. Yan, X. Zhang, S. Zhou, X. Xie, Y. Luo, and Y. Yu, Synthesis of WO₃ nanoparticles for photocatalytic O₂ evolution by thermal decomposition of ammonium tungstate loading on g-C₃N₄, Journal of Alloys and Compounds, 509, 2011, L232–L235.
- [27]. H. Y. He, Preparation and luminescence property of Sm-doped ZnWO₄ powders and films with wet chemical methods, Physica Status Solidi B, 246, 2009, 177–182.
- [28]. H. B. Fu, C. S. Pan, L. W. Zhang, and Y. F. Zhu, Synthesis, characterization and photocatalytic properties of nanosized Bi₂WO₆, PbWO₄ and ZnWO₄ catalysts, Materials Research Bulletin, 42, 2007, 696–706.
- [29]. J. X. Liu, X. L. Dong, X. W. Liu, F. Shi, S. Yin, and T. Sato, Solvothermal synthesis and characterization of tungsten oxides with controllable morphology and crystal phase, Journal of Alloys and Compounds, 509(5), 2011, 1482–1488.
- [30]. C. L. Yu and J. C. Yu, Sonochemical fabrication, characterization and photocatalytic properties of Ag/ZnWO₄ nanorod catalyst, Materials Science and Engineering: B, 164, 2009, 16–22.
- [31]. P. Belli, R. Bernabei, F. Cappella et al., Radioactive contamination of ZnWO₄ crystal scintillators, Nuclear Instruments and Methods in Physics Research A, 626–627(1), 2011, 31–38.
- [32]. F. G. Yang, Z. Y. You, and C. Y. Tu, End-pumping ZnWO₄:Tm³⁺ at ~ 1.9 μm eye-safe laser, Laser Physics Letters, 9, 2012, 204–206.
- [33]. V. V. Atuchin, E. N. Galashov, A. S. Kozhukhov, L. D. Pokrovsky, and V. N. Shlegel, Epitaxial growth of ZnO nanocrystals at ZnWO₄(0 1 0) cleaved surface, Journal of Crystal Growth, 318(1), 2011, 1147–1150.
- [34]. V. V. Atuchin, E. N. Galashov, O. Y. Khyzhun, A. S. Kozhukhov, L. D. Pokrovsky, and V. N. Shlegel, Structural and electronic properties of ZnWO₄(010) cleaved surface, Crystal Growth and Design, 11(6), 2011, 2479–2484.

Table 1: Typical run for the three semiconductors

WO₃		BaWO₄		Ba₃Y₂WO₉	
pH = 7.8 Dye concentration = 5×10^{-6} M Catalyst = 0.12g Light intensity = 37mWcm ⁻²		pH = 7.3 Dye concentration = 4×10^{-5} M Catalyst = 0.18g Light intensity = 37mWcm ⁻²		pH = 7.3 Dye concentration = 5×10^{-6} M Catalyst = 0.12g Light intensity = 37mWcm ⁻²	
Time	1+log O.D.	Time	1+log O.D.	Time	1+log O.D.
0.0 min.	0.5263	0.0 min.	0.4232	0.0 min.	0.4393
15.0 min.	0.5105	15.0 min.	0.3961	2.0 min.	0.3802
30.0 min.	0.4814	30.0 min.	0.3765	4.0 min.	0.3654
45.0 min.	0.4424	45.0 min.	0.3729	6.0 min.	0.3096
60.0 min.	0.4183	60.0 min.	0.3560	8.0 min.	0.2600
75.0 min.	0.3783	75.0 min.	0.3443	10.0 min.	0.2227
90.0 min.	0.3424	90.0 min.	0.3404	12.0 min.	0.1760
105.0 min.	0.3010	105.0 min.	0.3201	14.0 min.	0.1398
120.0 min.	0.2764	120.0 min.	0.2380	16.0 min.	0.1003
135.0 min.	0.2479	135.0 min.	0.2380	18.0 min.	0.0755

Table: 2 Comparative study of degradation of Azure-B:

Factors	WO ₃	BaWO ₄	Ba ₃ Y ₂ WO ₉
	Rate Constant = 9.2×10^{-5} sec ⁻¹	Rate Constant = 4.9×10^{-5} sec ⁻¹	Rate Constant = 8.44×10^{-4} sec ⁻¹
pH	7.8	7.3	7.3
Concentration of dye (moles/liter)	5×10^{-6}	4×10^{-6}	5×10^{-6}
Amount of semiconductor (g)	0.12	0.18	0.12
Intensity of light (mW/cm ²)	37	37	37

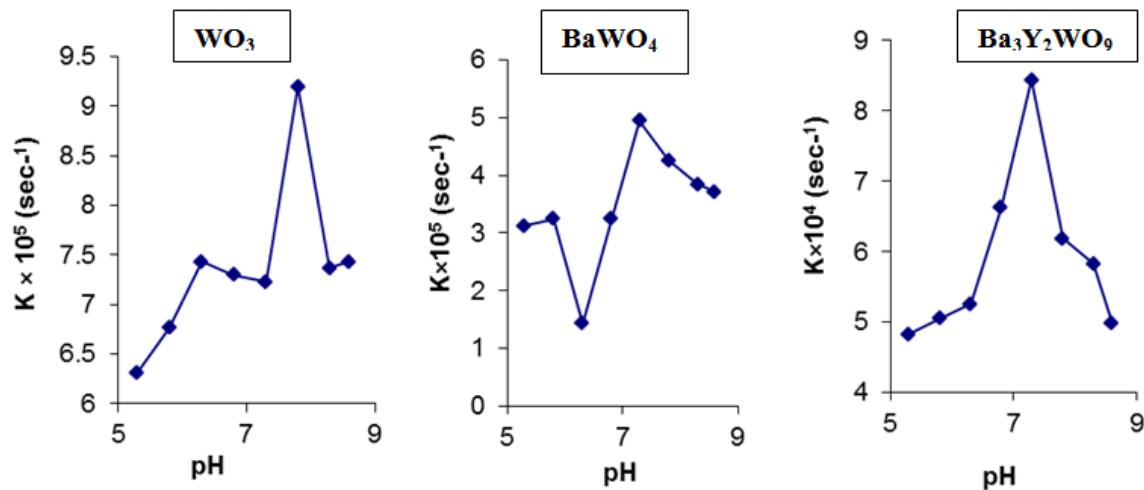


Figure 2: A comparative study of pH

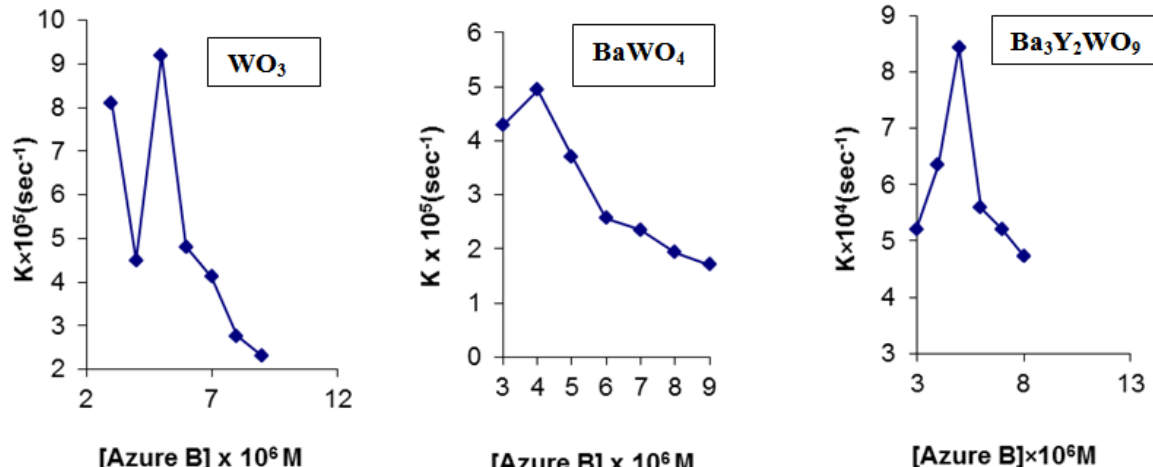


Figure 3: A comparative study of concentration of dye

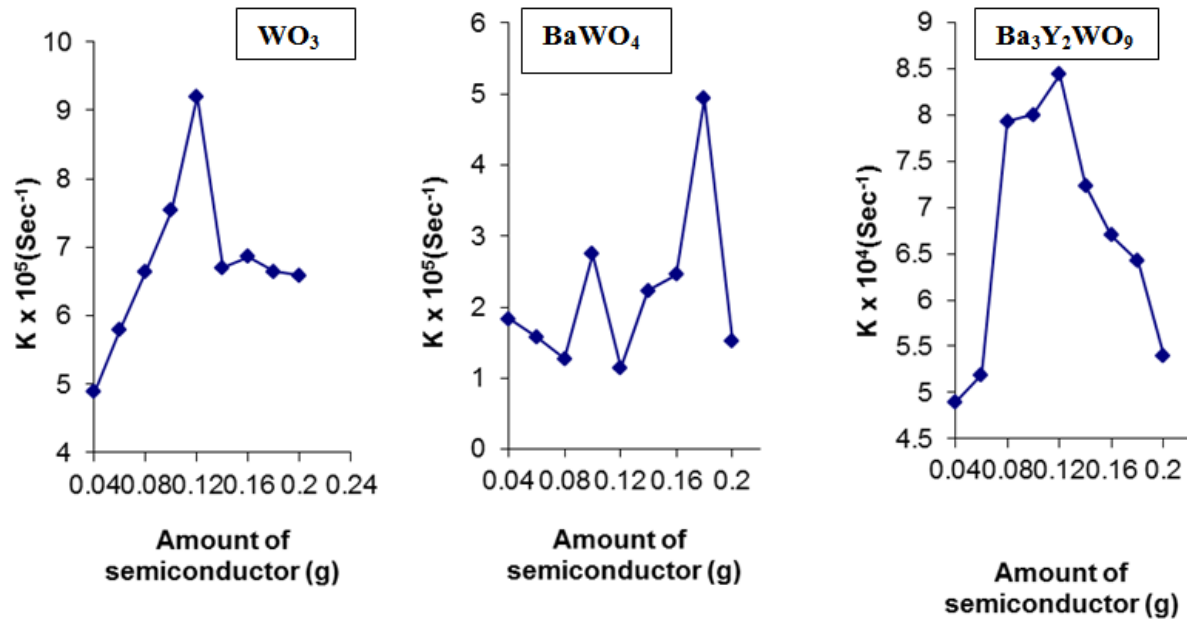


Figure 4: A comparative study of amount of semiconductor

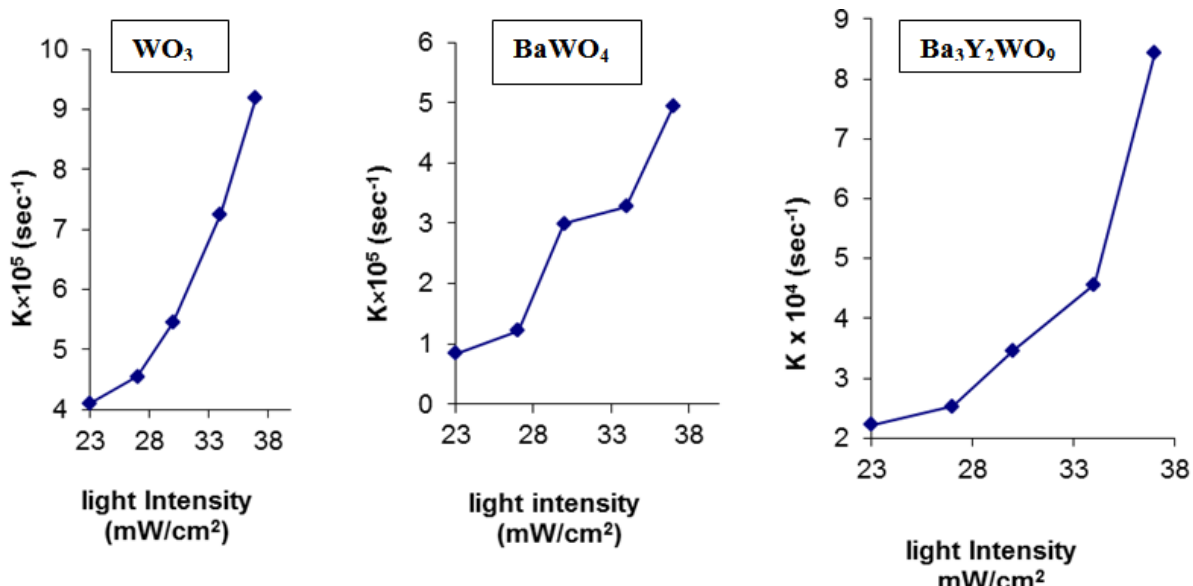


Figure 5: A comparative study of intensity of light

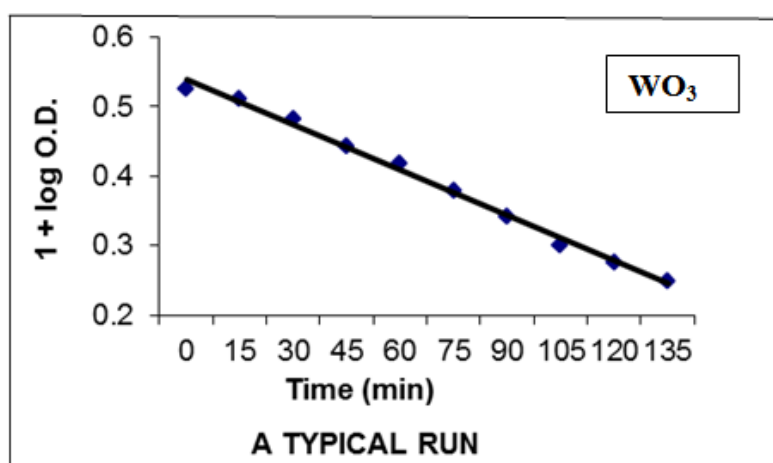


Figure 6: A typical run for WO_3 and Azure B

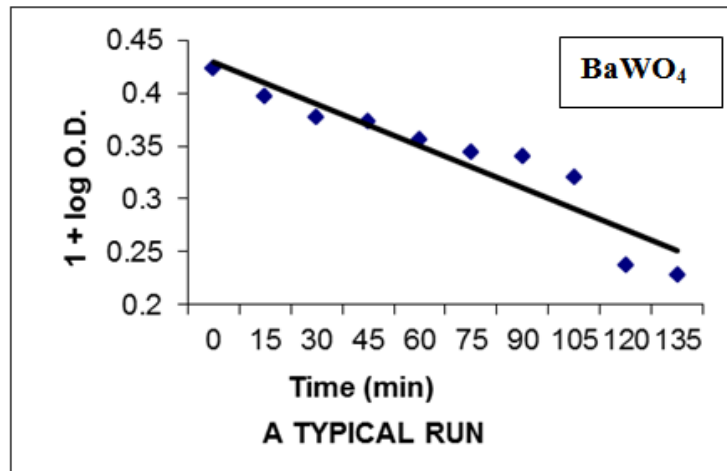


Figure 7: A typical run for BaWO₄ and Azure B

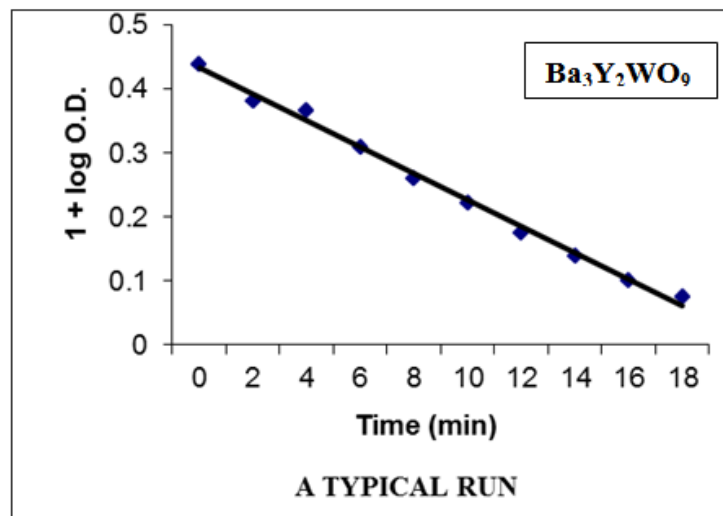


Figure 8: A typical run for Ba₃Y₂WO₉ and Azure B